A CLOSED-FORM ANALYTICAL MODEL AND SIMULATION OF SWITCHED RELUCTANCE MOTORS

I. A. M. ABDEL-HALIM H. G. HAMED O. E. S. Mohammed
Faculty of Engineering (Shoubra), Zagazig University, Benha Branch, 108 Shoubra street, Cairo, Egypt

ABSTRACT

In this paper, a closed-form analytical model of the unsaturated SRM from which its steady-state performance can be directly obtained is proposed. This model is used to simulate the SRM using the software package MATLAB/ SIMULINK. The model is validated by comparing the obtained results with previously published results.

نموذج رياضي و المحاكاة لمحركات الممانعة المتغيرة

إبراهيم عبد المنعم عبد الحليم حامد جلال حامد عمر السيد محمد
كلية الهندسة بشبرا - جامعة الزقازيق (فرع بنها)

ملخص البحث:

فى هذا البحث تم استنتاج نموذج رياضي يمكن الحصول منه على الأداء المستقر لمحرك الممانعة المتغيرة (switched reluctance motor) و ذلك في حالة عدم التشبع المغناطيسي لدائرته المغناطيسية . و قد تم استخدام هذا النموذج الرياضي في محاكاة المحرك و ذلك باستخدام برنامج المحاكاة (MATLAB/ SIMULINK) . و قد تم التحقق من صحة هذا النموذج الرياضي و ذلك بمقارنة النتائج التي تم الحصول عليها من عملية المحاكاة بنتائج أخرى سبق نشرها.

1. INTRODUCTION

Switched reluctance motors (SRMs) have many advantages such as simple mechanical construction and robustness [1], low manufacturing cost [2] and fast dynamic response [3]. It consists of a stator and a rotor, which are both laminated and have salient poles, and only the stator has windings on its poles [4]. Previous investigations have been conducted regarding modeling of the SRM [4, 5] and its simulation using the software package MATLAB/ SIMULINK [6]. However, there are

some items that had not received an in depth attention, such as modeling of the unsaturated SRMs by closed form equations at steady state taking into consideration the effect of phase resistance and not approximating the waveforms of the inductance-rotor position. Also, in previously published investigations, simulation of the unsaturated SRM at steady state using MATLAB/ SIMULINK have not been dealt with.

In this paper, closed-form equations for modeling the unsaturated SRM from which its steady-state performance can be obtained directly are proposed, and these equations are suitable for different inductance-rotor position waveforms. Also, these closed-form equations are simulated using the simulation package MATLAB/ SIMULINK [7]. The proposed model was validated by comparison between the obtained results and previously published results.

2. MODELING OF THE SRM UNDER STEADY-STATE CONDITIONS

2.1 Phase Inductance

Fig. (1) shows a four-phase 8/6 SR motor whose phases are (A, B, C and D), where β_s and β_r are, respectively, the stator and rotor pole arcs in mechanical radians, and Fig. (2) shows the waveform of the phase inductance. The mechanical angle (θ_m) and the electrical angle (θ) are related by [8]:

$$\theta = N_r\, \theta_m$$

where N_r is the number of rotor poles.

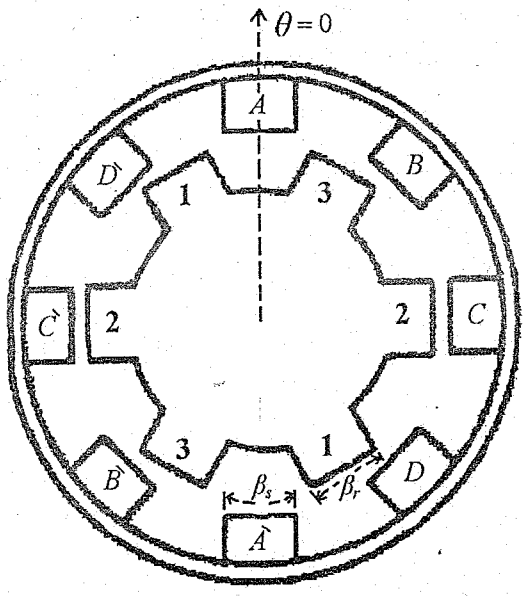

Fig. (1) Four-phase (8/6) SRM

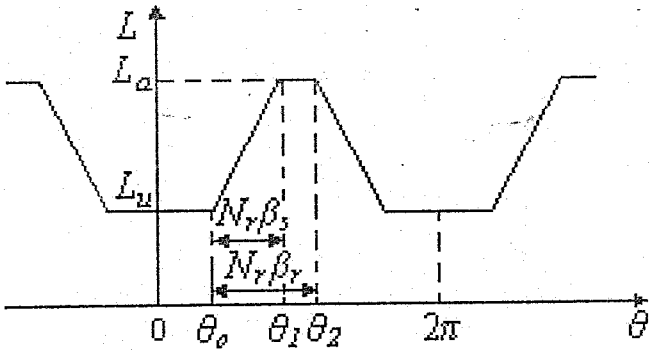

Fig. (2) Phase inductance waveform

In Fig. (2), the upper flat zone (L_a) of the inductance waveform is due to the complete overlapping between the stator phase poles and rotor poles, with the stator pole arc smaller than the rotor pole arc. The lower flat zone (L_u) is due to the absence of overlapping between rotor poles and the stator poles corresponding to that phase. Thus, the phase inductance can be expressed by:

$$L(\theta) = L_u \qquad 0 \le \theta \le \theta_o \quad (1)$$
$$L(\theta) = C_1\,\theta - C_2 \qquad \theta_o \le \theta \le \theta_1 \quad (2)$$
$$L(\theta) = L_a \qquad \theta_1 \le \theta \le \theta_2 \quad (3)$$
$$L(\theta) = -C_1\,\theta - C_3 \qquad \theta_2 \le \theta \le 2\pi - \theta_o \quad (4)$$
$$L(\theta) = L_u \qquad 2\pi - \theta_o \le \theta \le 2\pi \quad (5)$$

where the expressions of C_1 , C_2 , C_3 , θ_o , θ_1 and θ_2 are given in Appendix (A).
For an m-phase SR motor, the inductance of the k^{th} phase is given by [9]:

$$L_k(\theta) = L(\theta - \frac{k-1}{m}\,2\pi) \tag{6}$$

2.2 Phase Current

Considering an m-phase SR motor, the voltage equation of one phase is given by:

$$u_s = R\,i + \frac{d\lambda(i,\theta)}{dt} \tag{7}$$

where (u_s) is the applied voltage on the motor phase, (R) is the motor phase resistance and $\lambda(i,\theta)$ is the flux linkage as function of (i,θ) where (i) is the motor phase current. Since saturation of the magnetic circuit of the motor is not taken into consideration, the flux linkage of this phase can be expressed by:

$$\lambda(i,\theta) = L(\theta)\,i \tag{8}$$

Thus, eqn. (7) becomes:

$$u_s = R\,i + L(\theta)\frac{di}{d\theta}\frac{d\theta}{dt} + i\frac{dL(\theta)}{d\theta}\frac{d\theta}{dt} \tag{9}$$

When the motor is operating at steady state (i.e. at a steady-state average speed, ω), and since the speed of the motor is related to the rotor position by:

$$\frac{d\theta}{dt} = \omega \tag{10}$$

where ω is in (elec. rad/s) and θ is the rotor position in electrical radians, then, eqn. (9) becomes:

$$u_s = (R + \omega\frac{dL(\theta)}{d\theta})\,i + L(\theta)\,\omega\frac{di}{d\theta} \tag{11}$$

The modes of operation of the SRM can be, basically, divided into two modes. The

period of the first mode is when the motor phase is connected to the DC supply voltage (U_s) and its current is building up. The period of the second mode of operation begins when the current of the motor phase starts to decay, and the supply voltage applied to the phase winding under consideration is reversed, ($-U_s$). Thus, the electrical equation corresponding to the period of the first mode can be obtained as:

$$U_s = (R + \omega \frac{dL(\theta)}{d\theta})\, i + L(\theta)\, \omega \frac{di}{d\theta} \qquad (12)$$

and that corresponding to the period of the second mode can be obtained as:

$$-U_s = (R + \omega \frac{dL(\theta)}{d\theta})\, i + L(\theta)\, \omega \frac{di}{d\theta} \qquad (13)$$

Expressions for the building-up and decaying currents can be obtained by solving eqns. (12) and (13) respectively with the appropriate expressions of the phase inductance and the suitable initial values of the phase current are taken into consideration. The rotor position angle at which the building-up current starts is called the turn-on angle (θ_{on}), and that at which the decaying current starts is called the turn-off angle (β). The expressions of the phase current depend on the value of the turn-on angle (θ_{on}), which may be $\theta_{on} < \theta_o$ or $\theta_{on} \geq \theta_o$, and also on the value of the turn-off angle (β), which may be $\beta < \theta_1$ or $\beta = \theta_1$. Fig. (3) shows a typical waveform of the phase current when $\theta_{on} < \theta_o$ and $\beta < \theta_1$.

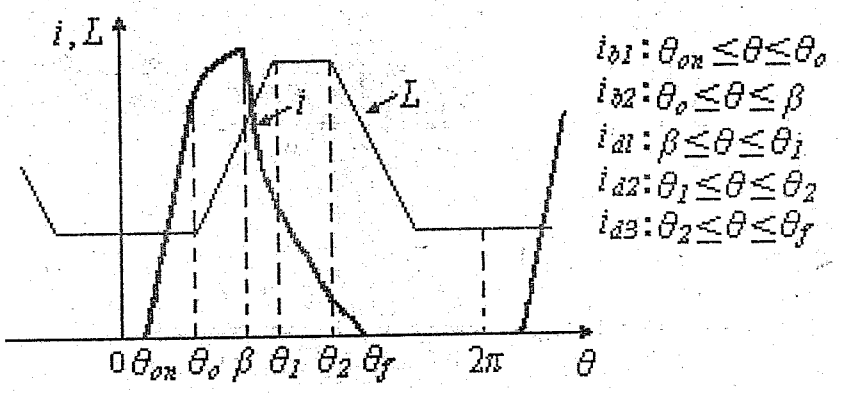

Fig. (3) Phase current and phase inductance waveforms ($\theta_{on} < \theta_o$ and $\beta < \theta_1$)

Therefore, the expressions of the phase current can be derived, using eqns. (12) and (13), as:

$$i_{b1}(\theta) = \frac{U_s}{R}\left[1 - e^{-(\theta - \theta_{on})R/(L_u \omega)}\right] \qquad \theta_{on} \leq \theta \leq \theta_o \qquad (14)$$

$$i_{b2}(\theta) = \frac{U_s}{R + C_1\omega} + \left[i_{b2o} - \frac{U_s}{R + C_1\omega} \right] \left[\frac{C_1\theta_o - C_2}{C_1\theta - C_2} \right]^{\frac{R + C_1\omega}{C_1\omega}} \qquad \theta_o \le \theta \le \beta \quad (15)$$

$$i_{d1}(\theta) = \frac{-U_s}{R + C_1\omega} + \left[i_{d1o} + \frac{U_s}{R + C_1\omega} \right] \left[\frac{C_1\beta - C_2}{C_1\theta - C_2} \right]^{\frac{R + C_1\omega}{C_1\omega}} \qquad \beta \le \theta \le \theta_1 \quad (16)$$

$$i_{d2}(\theta) = \frac{-U_s}{R} + [i_{d2o} + \frac{U_s}{R}]\, e^{-(\theta - \theta_1)R/(L_a\,\omega)} \qquad \theta_1 \le \theta \le \theta_2 \quad (17)$$

$$i_{d3}(\theta) = \frac{-U_s}{R - C_1\omega} + \left[i_{d3o} + \frac{U_s}{R - C_1\omega} \right] \left[\frac{-C_1\theta_2 - C_3}{-C_1\theta - C_3} \right]^{\frac{R - C_1\omega}{-C_1\omega}} \qquad \theta_2 \le \theta \le \theta_f \quad (18)$$

where

$$i_{b2o} = i_{b1}(\theta_o) = \frac{U_s}{R}\,[1 - e^{-(\theta_o - \theta_{on})R/(L_u\omega)}] \quad (19)$$

$$i_{d1o} = i_{b2}(\beta) = \frac{U_s}{R + C_1\omega} + \left[i_{b2o} - \frac{U_s}{R + C_1\omega} \right] \left[\frac{C_1\theta_o - C_2}{C_1\beta - C_2} \right]^{\frac{R + C_1\omega}{C_1\omega}} \quad (20)$$

$$i_{d2o} = i_{d1}(\theta_1) = \frac{-U_s}{R + C_1\omega} + \left[i_{d1o} + \frac{U_s}{R + C_1\omega} \right] \left[\frac{C_1\beta - C_2}{C_1\theta_1 - C_2} \right]^{\frac{R + C_1\omega}{C_1\omega}} \quad (21)$$

$$i_{d3o} = i_{d2}(\theta_2) = \frac{-U_s}{R} + [i_{d2o} + \frac{U_s}{R}]\, e^{-(\theta_2 - \theta_1)R/(L_a\,\omega)} \quad (22)$$

where i_{b1} and i_{b2} are the expressions of the phase current for the building-up period and i_{d1} , i_{d2} and i_{d3} are the expressions of the current for the decaying period. θ_f is the final angle at which the decaying current reaches zero.
When $\theta_{on} < \theta_o$ and $\beta = \theta_1$, the typical waveform of the phase current will be as shown in Fig. (4).

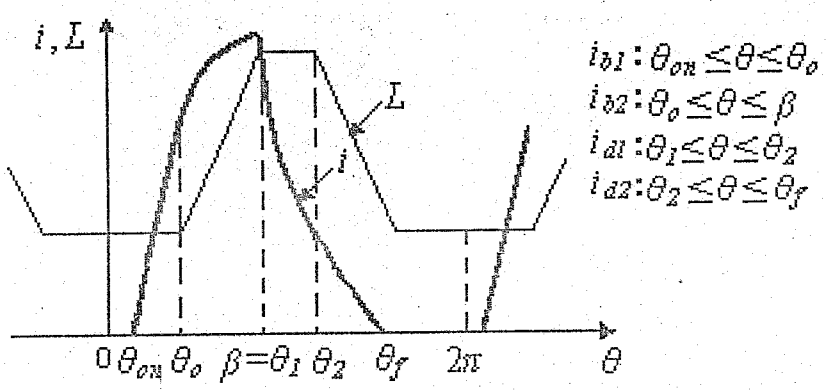

Fig. (4) Phase current and phase inductance waveforms ($\theta_{on} < \theta_o$ and $\beta = \theta_1$)

In this case, the expressions of i_{b1} and i_{b2} will be as eqns. (14) and (15) respectively. The expressions of the decaying currents i_{d1} and i_{d2} are derived as:

$$i_{d1}(\theta) = \frac{-U_s}{R} + [i_{d1o} + \frac{U_s}{R}]\, e^{-(\theta-\theta_1)R/(L_a\,\omega)} \qquad \beta \le \theta \le \theta_2 \quad (23)$$

$$i_{d2}(\theta) = \frac{-U_s}{R - C_1\omega} + \left[i_{d2o} + \frac{U_s}{R - C_1\omega}\right]\left[\frac{-C_1\theta_2 - C_3}{-C_1\theta - C_3}\right]^{\frac{R - C_1\omega}{-C_1\omega}} \qquad \theta_2 \le \theta \le \theta_f \quad (24)$$

where

$$i_{d1o} = i_{b2}(\beta) = \frac{U_s}{R + C_1\omega} + \left[i_{b2o} - \frac{U_s}{R + C_1\omega}\right]\left[\frac{C_1\theta_o - C_2}{C_1\beta - C_2}\right]^{\frac{R + C_1\omega}{C_1\omega}} \quad (25)$$

$$i_{d2o} = i_{d1}(\theta_2) = \frac{-U_s}{R} + [i_{d1o} + \frac{U_s}{R}]\, e^{-(\theta_2-\theta_1)R/(L_a\,\omega)} \quad (26)$$

When $\theta_{on} \ge \theta_o$ and $\beta < \theta_1$, the typical waveform of the phase current will be as shown in Fig. (5).

Therefore, the expressions of the phase current are derived as:

$$i_b(\theta) = \frac{U_s}{R + C_1\omega}\left[1 - \left[\frac{C_1\theta_{on} - C_2}{C_1\theta - C_2}\right]^{\frac{R+C_1\omega}{C_1\omega}}\right] \qquad \theta_{on} \le \theta \le \beta \quad (27)$$

$$i_{d1}(\theta) = \frac{-U_s}{R + C_1\omega} + \left[i_{d1o} + \frac{U_s}{R + C_1\omega} \right] \left[\frac{C_1\beta - C_2}{C_1\theta - C_2} \right]^{\frac{R+C_1\omega}{C_1\omega}} \qquad \beta \le \theta \le \theta_1 \quad (28)$$

$$i_{d2}(\theta) = \frac{-U_s}{R} + [i_{d2o} + \frac{U_s}{R}]\, e^{-(\theta - \theta_1)R/(L_a\,\omega)} \qquad \theta_1 \le \theta \le \theta_2 \quad (29)$$

$$i_{d3}(\theta) = \frac{-U_s}{R - C_1\omega} + \left[i_{d3o} + \frac{U_s}{R - C_1\omega} \right] \left[\frac{-C_1\theta_2 - C_3}{-C_1\theta - C_3} \right]^{\frac{R - C_1\omega}{-C_1\omega}} \qquad \theta_2 \le \theta \le \theta_f \quad (30)$$

where

$$i_{d1o} = i_b(\beta) = \frac{U_s}{R + C_1\omega} \left[1 - \left[\frac{C_1\theta_{on} - C_2}{C_1\beta - C_2} \right]^{\frac{R+C_1\omega}{C_1\omega}} \right] \quad (31)$$

$$i_{d2o} = i_{d1}(\theta_1) = \frac{-U_s}{R + C_1\omega} + \left[i_{d1o} + \frac{U_s}{R + C_1\omega} \right] \left[\frac{C_1\beta - C_2}{C_1\theta_1 - C_2} \right]^{\frac{R+C_1\omega}{C_1\omega}} \quad (32)$$

$$i_{d3o} = i_{d2}(\theta_2) = \frac{-U_s}{R} + [i_{d2o} + \frac{U_s}{R}]\, e^{-(\theta_2 - \theta_1)R/(L_a\,\omega)} \quad (33)$$

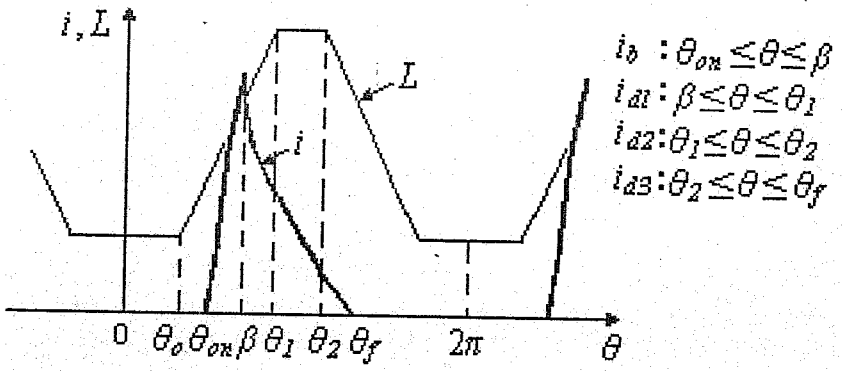

Fig. (5) Phase current and phase inductance waveforms ($\theta_{on} \ge \theta_o$ and $\beta < \theta_1$)

When $\theta_{on} \geq \theta_o$ and $\beta = \theta_1$, the typical waveform of the phase current will be as shown in Fig. (6).

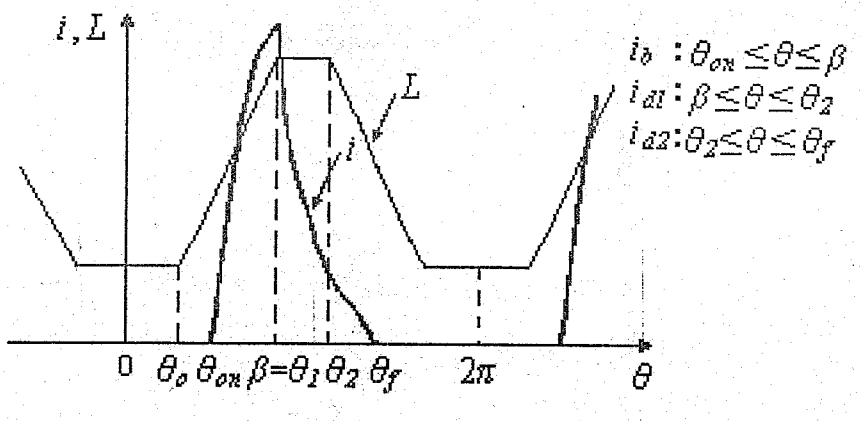

Fig. (6) Phase current and phase inductance waveforms ($\theta_{on} \geq \theta_o$ and $\beta = \theta_1$)

In this case, the expression of the building-up current (i_b) will be the same as that obtained in eqn. (21), and the expressions of the decaying current will be as follows:

$$i_{d1}(\theta) = \frac{-U_s}{R} + [i_b(\beta) + \frac{U_s}{R}]\, e^{-(\theta-\theta_1)R/(L_a\,\omega)} \qquad \beta \leq \theta \leq \theta_2 \quad (34)$$

$$i_{d2}(\theta) = \frac{-U_s}{R - C_1\omega} + \left[i_{d1}(\theta_2) + \frac{U_s}{R - C_1\omega} \right] \left[\frac{-C_1\theta_2 - C_3}{-C_1\theta - C_3} \right]^{\frac{R - C_1\omega}{-C_1\omega}} \qquad \theta_2 \leq \theta \leq \theta_f \quad (35)$$

where

$$i_{d1o} = i_b(\beta) = \frac{U_s}{R + C_1\omega} \left[1 - \left[\frac{C_1\theta_{on} - C_2}{C_1\beta - C_2} \right]^{\frac{R + C_1\omega}{C_1\omega}} \right] \quad (36)$$

$$i_{d2o} = i_{d1}(\theta_2) = \frac{-U_s}{R} + [i_{d1o} + \frac{U_s}{R}]\, e^{-(\theta_2-\theta_1)R/(L_a\,\omega)} \quad (37)$$

2.3 Developed Torque

The developed phase torque of the SRM is given by [10]:

$$T(i,\theta) = \frac{N_r}{2} i^2 \frac{dL}{d\theta} \tag{38}$$

For a SR motor with m phases, the total electromagnetic torque developed is obtained from:

$$T_e = \sum_{k=1}^{m} T_k = \frac{N_r}{2} \sum_{k=1}^{m} (i_k)^2 \frac{dL_k(\theta)}{d\theta} \tag{39}$$

where L_k is the inductance of the k^{th} phase obtained from eqn. (6) and (i_k) is its current.

3. SIMULATION OF SWITCHED RELUCTANCE MOTOR

The analytical model of the SRM at steady state without taken the effect of saturation into consideration, derived in Section 2, is used to simulate the motor using the simulation package MATLAB/ SIMULINK [7].

The following algorithm is applied to obtain the required simulation:

Depending on the value of θ_{on}, $\theta_{on} < \theta_o$ or $\theta_{on} \geq \theta_o$, and the value of β, $\beta < \theta_1$ or $\beta = \theta_1$, where θ_o and θ_1 are as shown in Fig. (2), we choose the appropriate equations of the current.

For $\theta_{on} < \theta_o$, eqn. (14), the equation of i_{b1}, for the range $\theta_{on} \leq \theta \leq \theta_o$ is used and eqn. (15), the equation of i_{b2}, for the range $\theta_o \leq \theta \leq \beta$ is used.

After the rotor position β, if β is less than θ_1, Fig. (3), i_{d1}, eqn. (16), is used in the range $\beta \leq \theta \leq \theta_1$ as long as the phase current is greater than zero. If the current reaches a zero value before $\theta = \theta_1$, then $\theta_f < \theta_1$, and if not, the equation of i_{d2}, eqn. (17), is used in the range $\theta_1 \leq \theta \leq \theta_2$. Also, in this case, if i_{d2} reaches zero value before θ_2, then $\theta_f < \theta_2$, and if not, then the equation of i_{d3}, eqn. (18), is used in the range $\theta_2 \leq \theta \leq \theta_f$.

If $\beta = \theta_1$, Fig. (4), the equation of i_{d1}, eqn. (23), is used in the range $\beta \leq \theta \leq \theta_2$. If the current does not reach a zero value before θ_2, then the equation of i_{d2}, eqn. (24), is used in the range $\theta_2 \leq \theta \leq \theta_f$.

When $\theta_{on} \geq \theta_o$, then eqn. (27), the equation of i_b, is used in the range $\theta_{on} \leq \theta \leq \beta$.

Also, eqns. (28), (29) and (30) are used instead of eqns. (16), (17) and (18) respectively for $\beta < \theta_1$, and eqns. (34) and (35) are used respectively instead of eqns. (23) and (24) for $\beta = \theta_1$.

It should be noted that if $\beta_s = \beta_r$, then the equations corresponding to the range $\theta_1 \leq \theta \leq \theta_2$ would not be needed.

To obtain the corresponding values of the phase torque, eqn. (38) is used with the appropriate values of $dL/d\theta$, and the total developed torque can be obtained from eqn. (39).

The SIMULINK block diagram for a three-phase (6/4) motor, whose data is given in Appendix (B), at steady state is shown in Fig. (7).

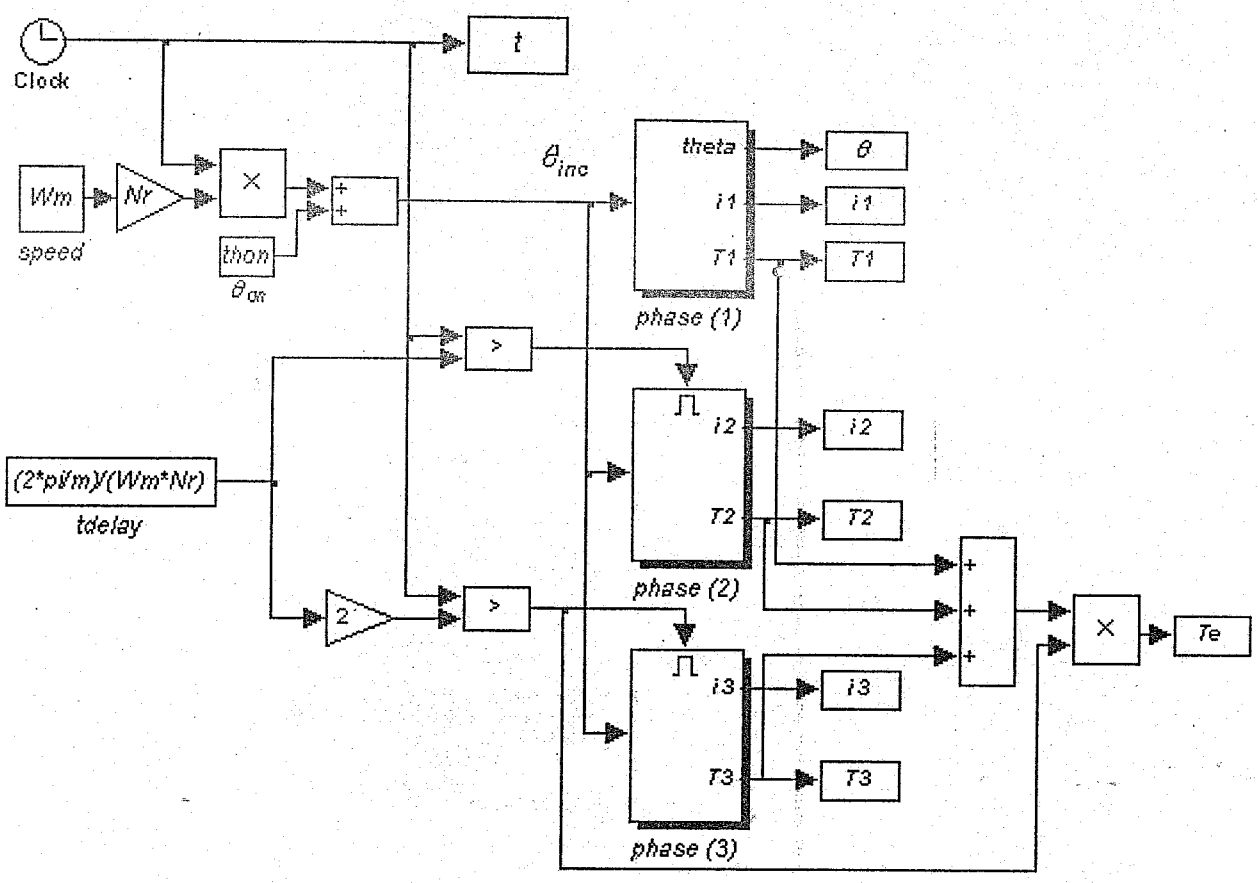

Fig. (7) Block diagram of (6/4) SRM for the unsaturated steady-state case (Shadowed blocks are subsystems)

The data required for this block diagram is obtained from a data file given in Appendix (C). The details of the block diagram are as follows:
The block 'tdelay', where the number of motor phases (m) is three and the number of rotor poles (N_r) is four, gives the required time delay, corresponding to 120 ° elec., between the subsystems 'phase (2)' and 'phase (1)'. Also, the output of 'tdelay' is multiplied by 2 to give the time delay, corresponding to 240 ° elec., between the subsystems 'phase (3)' and 'phase (1)'. The currents i_1, i_2 and i_3, and the developed torques T_1, T_2 and T_3 of phase (1), phase (2) and phase (3) respectively are obtained from the subsystems corresponding to these phases. The computation of the steady-state total developed torque starts at the end of the time delay corresponding to 240° elec.
It should be noted that the shadowed blocks in Fig. (7) and in the subsequent figures represent subsystem blocks. Also, the symbol θ is the absolute value of the rotor position angle and θ_{inc} is the incremental, accumulated, value.
The details of the subsystem 'phase (1)', corresponding to the case in which ($\beta_s \neq \beta_r$), is shown in Fig. (8). The 'phase (2)' and 'phase (3)' subsystems have similar constructions except that the input rotor position to the block 'phase (2)' is decreased by the angle ($2\pi/3$), and the input rotor position to 'phase (3)' is decreased by the angle ($4\pi/3$).
Each phase block contains the subsystems 'I', 'II', 'III', 'IV' and 'V' and they will operate according to the explained algorithm as shown in Table (1). Each of these subsystems gives the phase current and the phase torque when its conditions of operation are obtained by checking the value of the rotor position and the phase current as shown at the left hand side of Fig. (8).

The current '*io*' shown on each block of the subsystems 'I', 'II', 'III', 'IV' and 'V' is the initial value of the current of its corresponding subsystem.
The subsystems 'I', 'II', 'III', 'IV' and 'V' are shown in Figs. (9) to (13). Also, the details of the subsystems 'C_1', 'C_2' and 'C_3' are shown in Fig. (14), and the details of the subsystems 'subsystem (1)', 'subsystem (2)', 'θ_o', 'θ_1' and 'θ_2', are shown in Fig. (15).

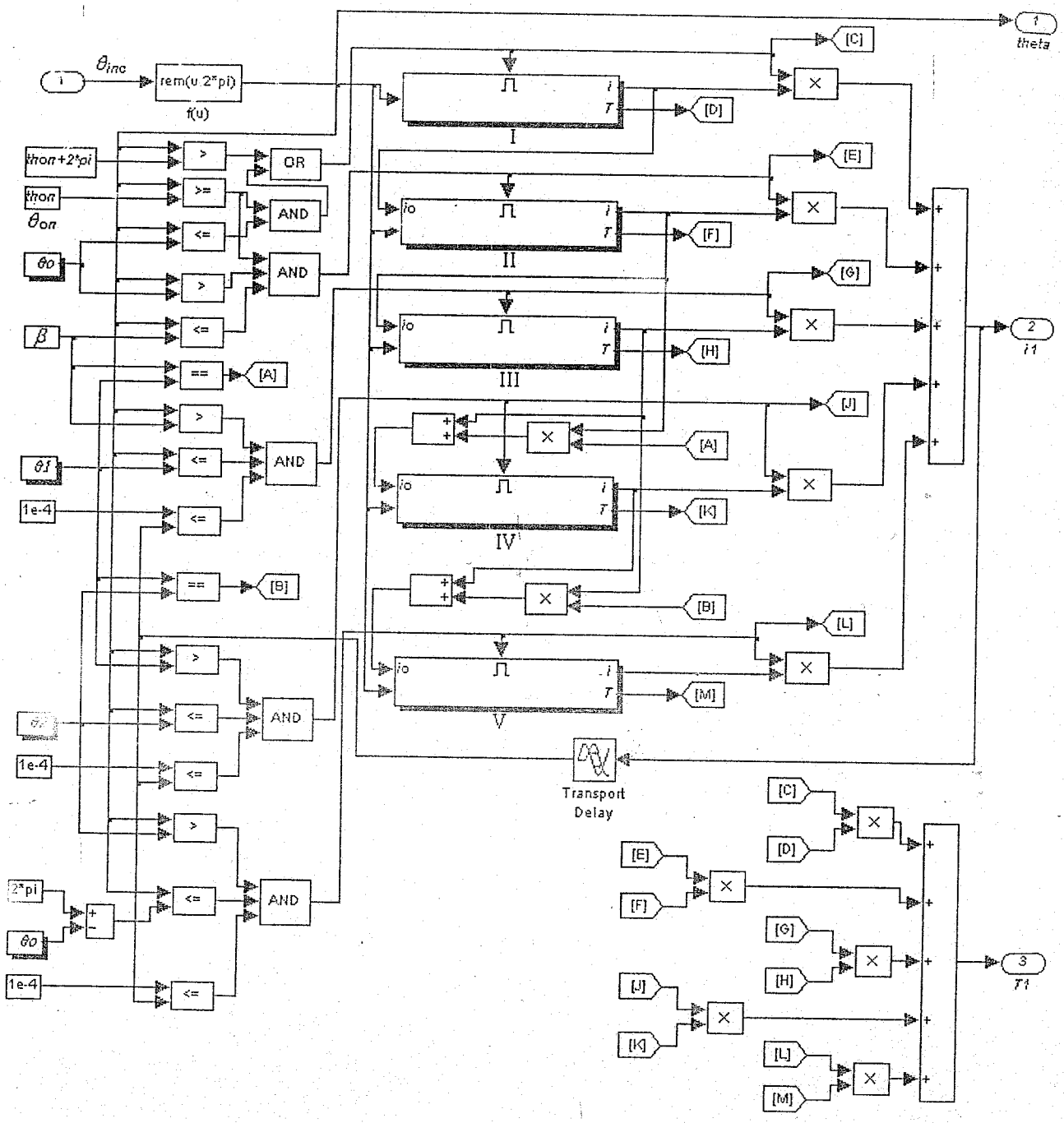

Fig. (8) Block diagram of the subsystem 'phase (1)'
(Shadowed blocks are subsystems)

Table (1)

Sub-system	Corresponding equations for each subsystem according to the values of θ_{on} and β			
	$\theta_{on} < \theta_o$ and $\beta < \theta_1$	$\theta_{on} < \theta_o$ and $\beta = \theta_1$	$\theta_{on} \geq \theta_o$ and $\beta < \theta_1$	$\theta_{on} \geq \theta_o$ and $\beta = \theta_1$
I	$i_{b1}(\theta)$, eqn. (14), and $i_o = 0$	$i_{b1}(\theta)$, eqn. (14), and $i_o = 0$	—	—
II	$i_{b2}(\theta)$, eqn. (15), and $i_o = i_{b2o}$, eqn. (19)	$i_{b2}(\theta)$, eqn. (15), and $i_o = i_{b2o}$, eqn. (19)	$i_b(\theta)$, eqn. (27), and $i_o = 0$	$i_b(\theta)$, eqn. (27), and $i_o = 0$
III	$i_{d1}(\theta)$, eqn. (16), and $i_o = i_{d1o}$, eqn. (20)	—	$i_{d1}(\theta)$, eqn. (28), and $i_o = i_{d1o}$, eqn. (31)	—
IV	$i_{d2}(\theta)$, eqn. (17), and $i_o = i_{d2o}$, eqn. (21)	$i_{d1}(\theta)$, eqn. (23), and $i_o = i_{d1o}$, eqn. (25)	$i_{d2}(\theta)$, eqn. (29), and $i_o = i_{d2o}$, eqn. (32)	$i_{d1}(\theta)$, eqn. (34), and $i_o = i_{d1o}$, eqn. (36)
V	$i_{d3}(\theta)$, eqn. (18), and $i_o = i_{d3o}$, eqn. (22)	$i_{d2}(\theta)$, eqn. (24), and $i_o = i_{d2o}$, eqn. (26)	$i_{d3}(\theta)$, eqn. (30), and $i_o = i_{d3o}$, eqn. (33)	$i_{d2}(\theta)$, eqn. (35), and $i_o = i_{d2o}$, eqn. (37)

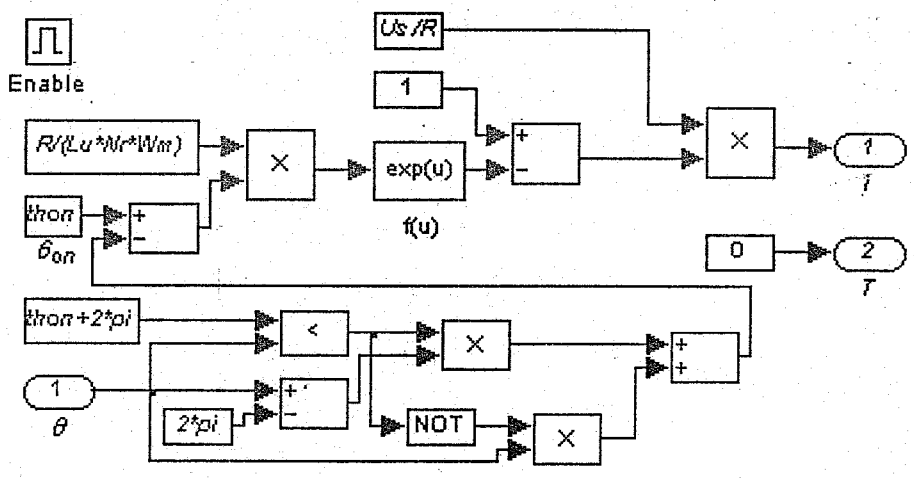

Fig. (9) Block diagram of the subsystem 'I'

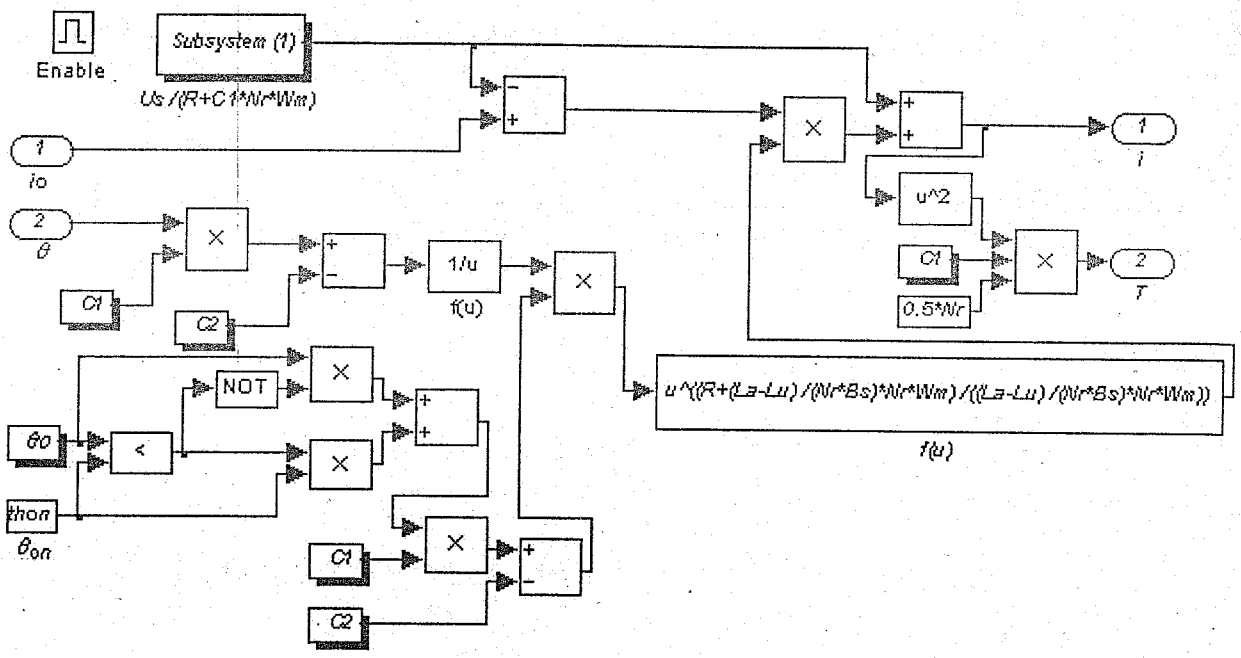

Fig. (10) Block diagram of the subsystem 'II'
(Shadowed blocks are subsystems)

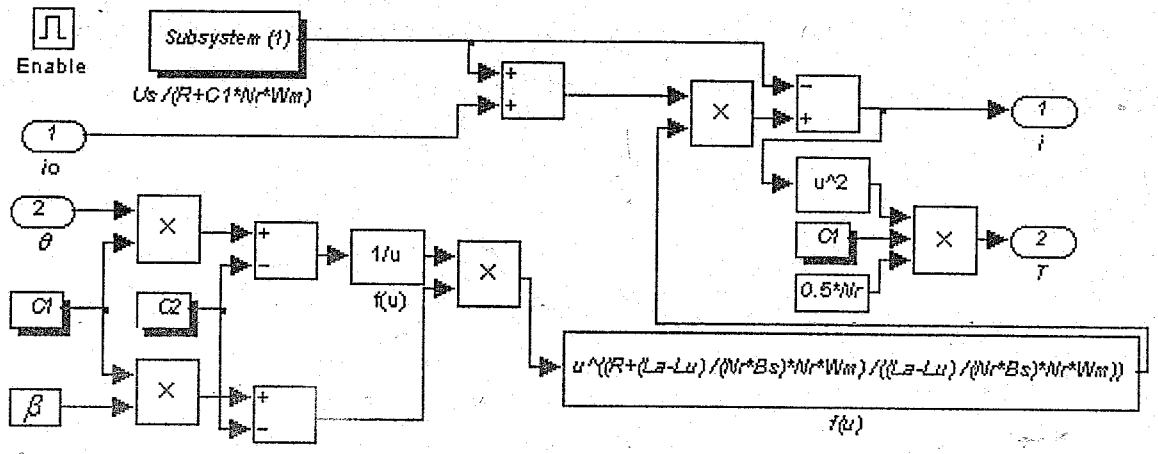

Fig. (11) Block diagram of the subsystem 'III'
(Shadowed blocks are subsystems)

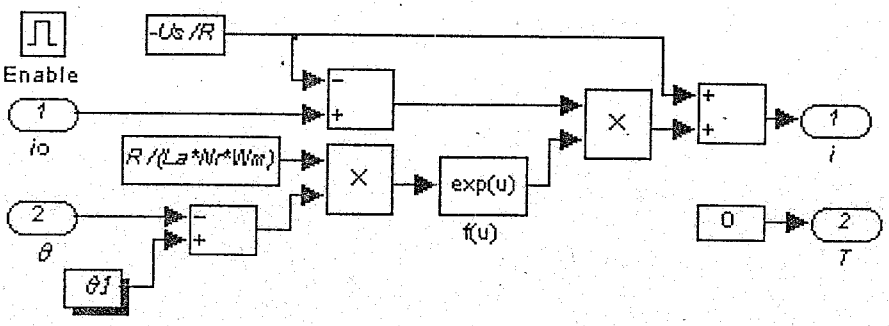

Fig. (12) Block diagram of the subsystem 'IV'
(Shadowed blocks are subsystems)

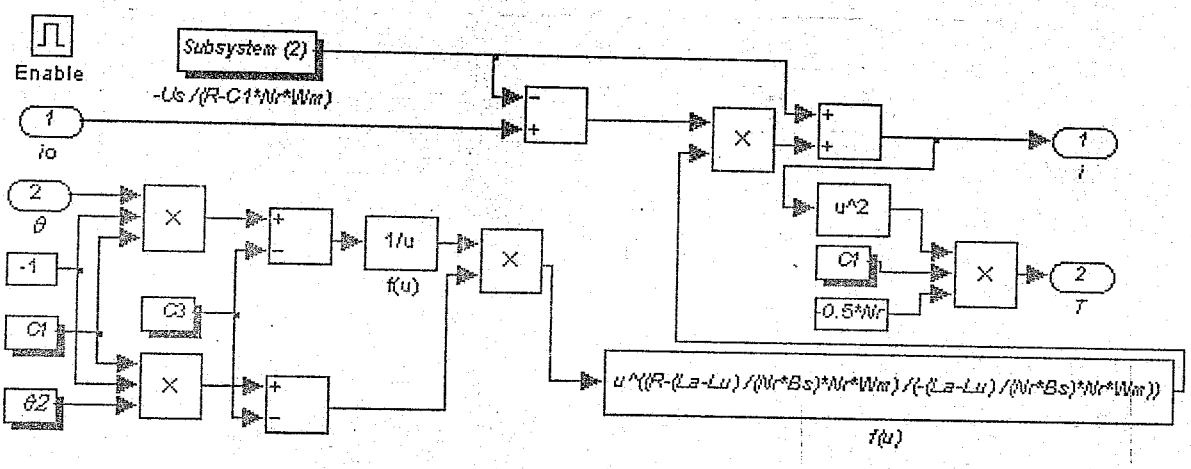

Fig. (13) Block diagram of the subsystem 'V'
(Shadowed blocks are subsystems)

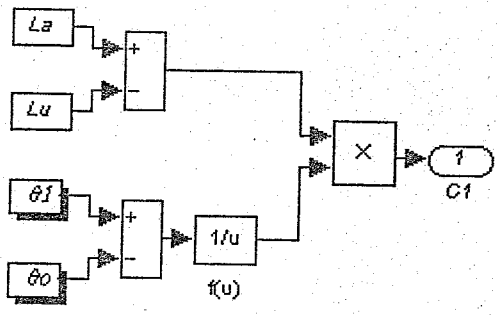

(a) 'C_1' subsystem

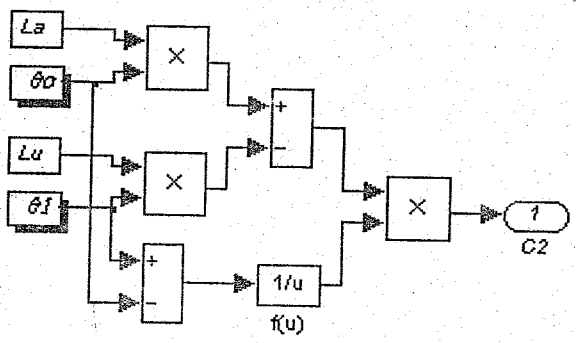

(b) 'C_2' subsystem

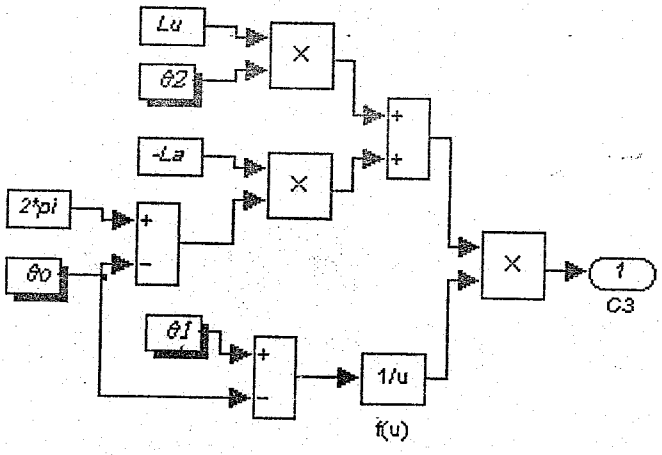

(c) 'C_3' subsystem

Fig. (14) Block diagrams of the subsystems 'C_1', 'C_2' and 'C_3'
(Shadowed blocks are subsystems)

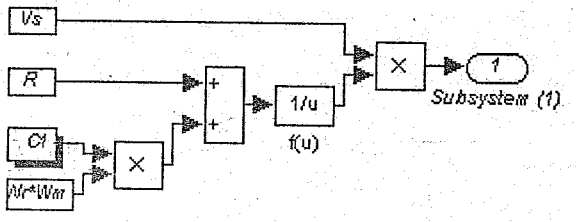

(a) 'Subsystem (1)' details

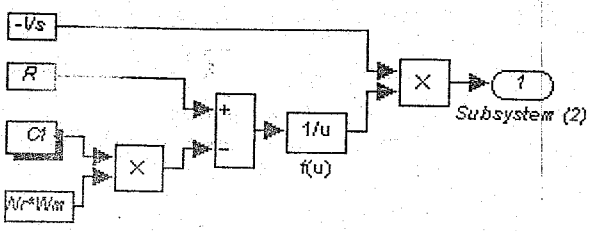

(b) 'Subsystem (2)' details

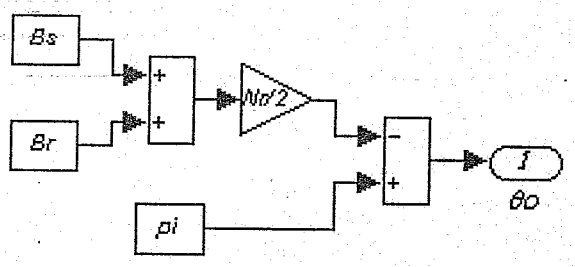

(c) 'θ_o' subsystem

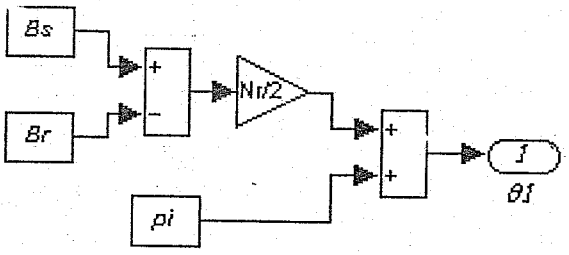

(d) 'θ_1' subsystem

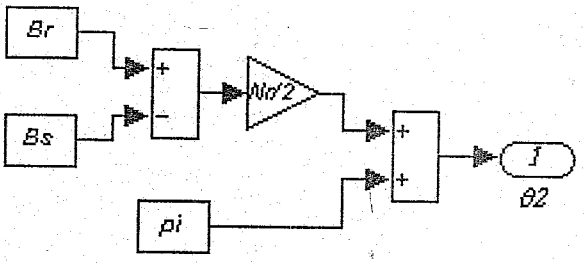

(e) 'θ_2' subsystem

Fig. (15) Block diagrams of different subsystems (Shadowed blocks are subsystems)

4. RESULTS

The results of the motor characteristics from this simulation are obtained at (U_s = 150 V, $\theta_{on} = 0$, $\beta = 120^\circ$ elec. and $n = 2214$ r.p.m) with the motor running at no load. The waveforms of the phase current, phase torque and total developed torque against rotor position were obtained and compared with the numerical results obtained in Reference [6], Figs. (16) to (18). From these figures, it is evident that the two sets of results are in close agreement.

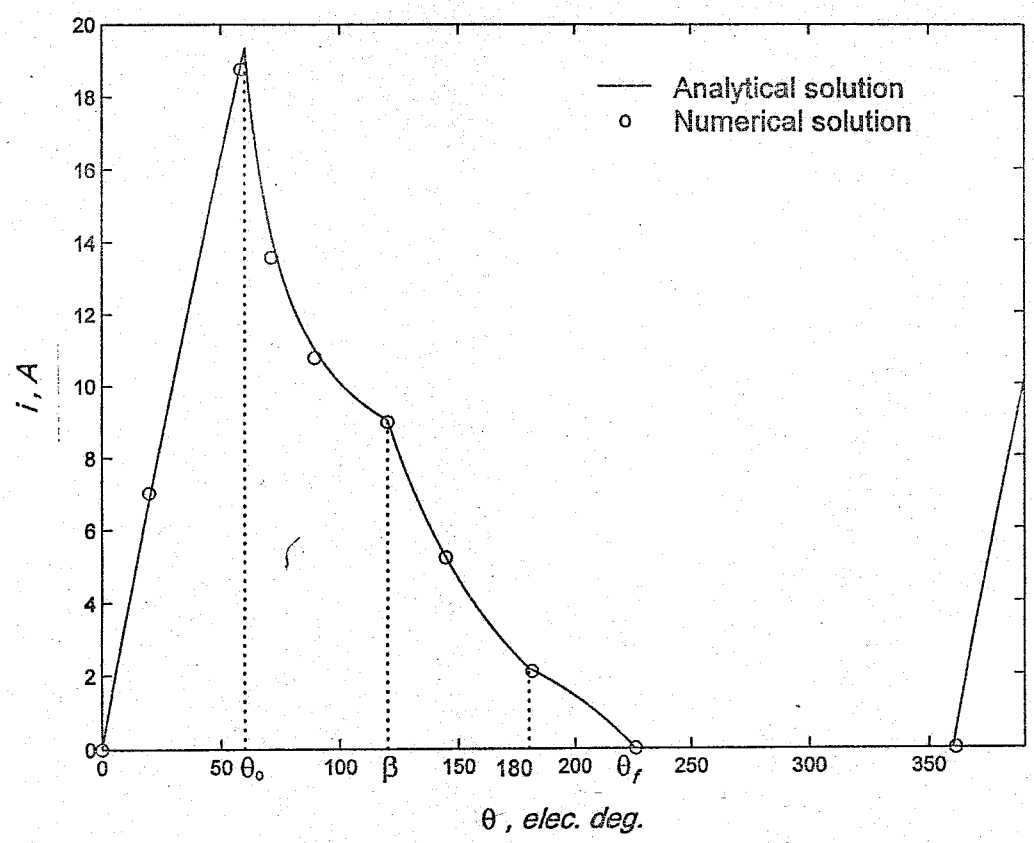

Fig. (16) Phase current versus rotor position
(U_s = 150 V, n = 2214 rpm, θ_{on} = 0° and β = 120°)

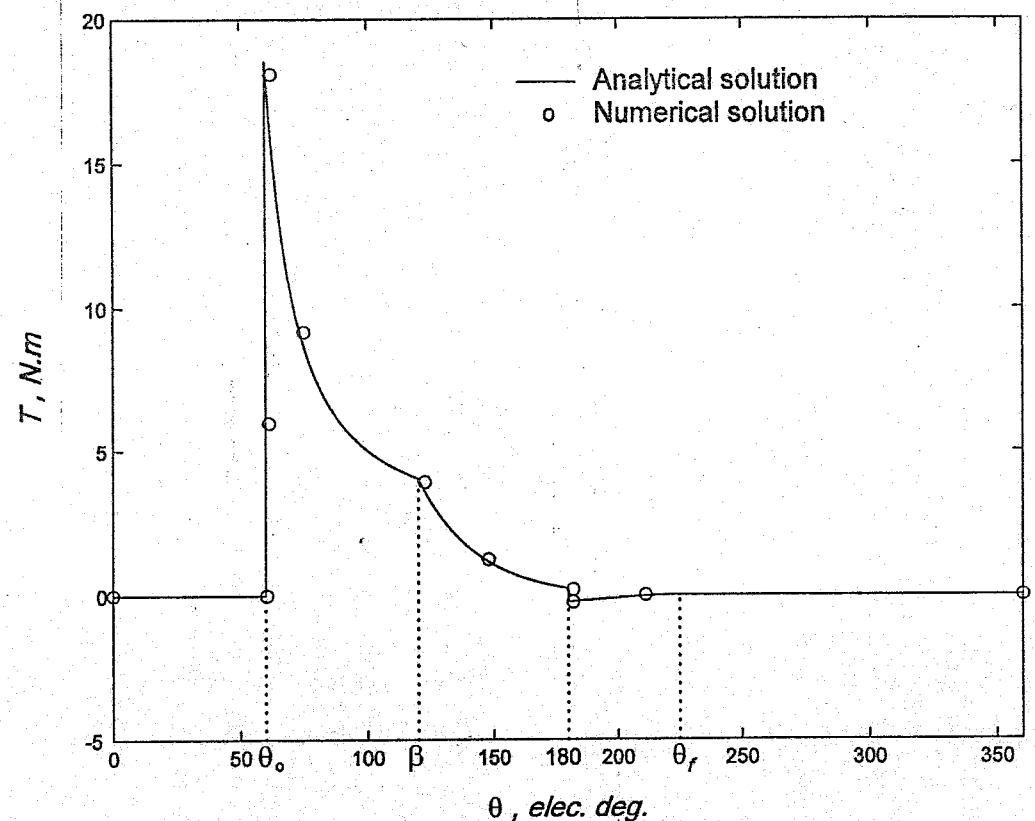

Fig. (17) Developed phase torque versus rotor position
(U_s = 150 V, n = 2214 rpm, θ_{on} = 0° and β = 120°)

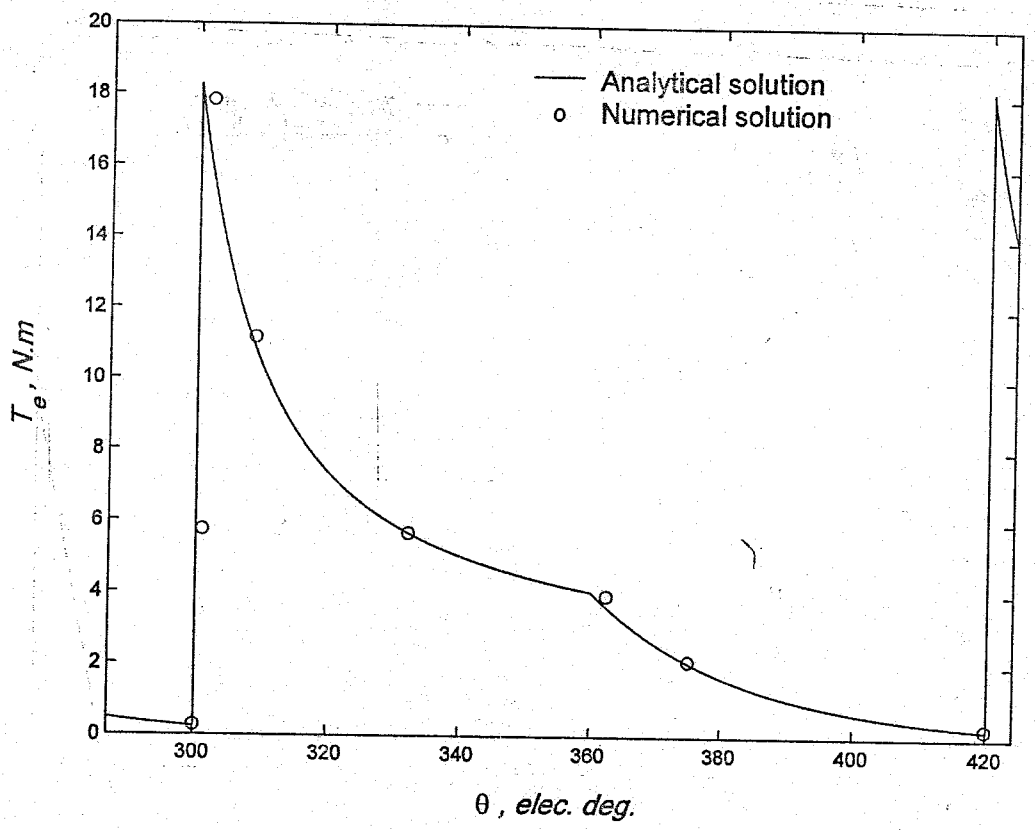

Fig. (18) Total developed torque versus rotor position ($U_s = 150$ V, $n = 2214$ p.u., $\theta_{on} = 0^\circ$ and $\beta = 120^\circ$)

5. CONCLUSION

A proposed analytical model for the unsaturated motor at steady state has been presented. This model is simulated by the software package (MATLAB/ SIMULINK), and it gives good results.

REFERENCES

[1] M. Stiebler and Ke Liu, "An analytical model of switched reluctance machines," IEEE Trans. Energy Conversion, vol. 14, no. 4, pp. 1100—1107, Dec. 1999.

[2] C. Sorandaru, N. Messina, and G. Atanasiu, "Optimum current control for a 8/6 switched reluctance motor using a TMS320C24x," in Proc. ELECTROMOTION'99, 3rd Int. Symp. Advanced Electromechanical Motion Systems, Patras, Greece, 1999, pp. 555—560.

[3] M. N. Anwar, I. Husain, and A. V. Radun, "A comprehensive design methodology for switched reluctance machines," IEEE Trans. Ind. Applicat., vol. 37, no. 6, pp.1684—1692, Nov./Dec. 2001.

[4] C.-C. Kim, J. Hur, and D.-S. Hyun, "Simulation of a switched reluctance motors using matlab / M-file," in Proc. IECON'02, 28th Ann. Conf. IEEE Ind. Electron. Soc., vol. 2, 2002, pp. 1066—1071.

[5] I. A. M. Abdel-Halim, H. G. Hamed, Kh. M. Hassaneen, and H. A. Mansour, "Performance analysis of switched reluctance motors," in Proc. MEPCON'2000, 7th Int. Middle-East Power Systems Conf. , Egypt, March 2000, pp. 169—174.

[6] F. Soares and P. J. C. Branco, "Simulation of a 6/4 switched reluctance motor based on Matlab/Simulink environment," IEEE Trans. Aerosp. Electron. Sys., vol. 37, no. 3, pp. 989—1009, July 2001.

[7] SIMULINK 3, The MathWorks, Inc., 1999.

[8] D. N. Essah and S. D. Sudhoff, "An improved analytical model for the switched reluctance motor," IEEE Trans. Energy Conversion, vol. 18, no. 3, pp. 349—356, Sep. 2003.

[9] B. K. Panda and P. K. Dash, "Application of nonlinear control to switched reluctance motors: a feedback linearisation approach," Proc. Inst. Elect. Eng.—Elect. Power Applicat., vol.143, no. 5, pp. 371–379, Sep. 1996.
[10] N. J. Nagel and R. D. Lorenz, "Modeling of a saturated switched reluctance motor using an operating point analysis and the unsaturated torque equation," IEEE Trans. Ind. Applicat., vol. 36, no. 3, pp. 714–721, May/June 2000.

Appendix (A)

$$C_1 = \frac{L_a - L_u}{\theta_1 - \theta_o}$$

$$C_2 = \frac{L_a\,\theta_o - L_u\,\theta_1}{\theta_1 - \theta_o}$$

$$C_3 = \frac{-L_a\,(2\pi - \theta_o) + L_u\,\theta_2}{\theta_1 - \theta_o}$$

$$\theta_o = \pi - N_r \frac{\beta_r + \beta_s}{2}$$

$$\theta_1 = \pi - N_r \frac{\beta_r - \beta_s}{2}$$

$$\theta_2 = \pi + N_r \frac{\beta_r - \beta_s}{2}$$

Appendix (B)

$R = 1.3\ \Omega$, $L_a = 60$ mH, $L_u = 8$mH, $N_r = 4$, $m = 3$, $\beta_s = \beta_r = \pi / 6$, $J = 0.0013$ Kg.m^2, $B = 0.0183$ N.m/(rad/s), $U_s = 150$ V.

Appendix (C)

```
% The data needed by the block diagram of Fig. (7).
clc
clear
R = 1.3 ; La = 60e-3  ; Lu = 8e-3 ; Nr = 4 ;  m = 3 ; Bs = pi/6; Br = pi/6 ;
% (Bs) and (Br) are the stator pole arc and the rotor pole arc respectively.
Us = 150 ; Wm = 231.87 ; thon = 0*Nr*pi/180 ; b = 30*Nr*pi/180;
% (thon) and (b) are the turn-on angle and the turn-off angle respectively.
```